Dynamics associated with Bose-Einstein statistics of orthoexcitons generated by resonant excitations in cuprous oxide

M. Y. Shen, T. Yokouchi, S. Koyama, and T. Goto
Department of Physics, Tohoku University, Sendai 980-77, Japan
(Received 3 July 1997; revised manuscript received 14 August 1997)

Orthoexcitonic gas in cuprous oxide is generated by one and two photon resonant excitations at different excitation intensities and at different temperatures between 1.8 and 4.2 K. The experimental results are analyzed by simulation with a Boltzmann equation. When the exciton density is low, the observed luminescence is found to originate from a nonequilibrium excitonic gas where the exciton-LA phonon scattering dominates. When the exciton density is very high, not only the exciton-LA phonon scattering but also the exciton-exciton scattering is important. The observed luminescence consists of two systems: one is from an exciton system that is distributed according to the usual Bose-Einstein statistics with chemical potential $\mu=0$, while the other is from excitons with zero kinetic energy. The two systems were found to be in thermal equilibrium. The latter system might be a form of Bose-Einstein condensation. [S0163-1829(97)05644-0]

I. INTRODUCTION

The laser cooling and trapping of atoms have recently resulted in the experimental realization of Bose-Einstein condensation (BEC) of cold atoms.[1] Similar results suggesting the existence of condensation effects were previously reported in a paraexcitonic gas of cuprous oxide.[2] The research of the exciton BEC in cuprous oxide began from research of Bose-Einstein statistical orthoexcitons.[3,4] Several attempts have been made to observe the BEC of the orthoexcitonic gas[4–7] under one-photon excitation. Since the temperature of the orthoexcitonic gas was always higher than the critical temperature for the BEC, under the one-photon excitation, BEC was not observed. The relaxation of photogenerated electron-hole pairs resulted in a temperature rise of the exciton gas up to about 100 K, and the density of the orthoexciton was saturated and always lower than the critical density for the BEC.[5,8] Hence, the BEC of the orthoexciton could not be realized by the one-phonon absorption method.

We[9] have recently created orthoexcitons kept at low temperature by two-photon resonant excitation. In the case of the two-photon resonant excitation, the temperature of the orthoexcitonic system could be maintained sufficiently low, which resulted in an exciton density high enough to allow us to study the quantum Bose-Einstein statistical properties of a nearly ideal Bose gas.

When the gas is observed on time scales long compared with the average scattering time of the particles, the kinetic energy distribution (Maxwell-Boltzmann, Fermi-Dirac, or Bose-Einstein) always has a well-defined temperature and a chemical potential. When the definite temperature and the chemical potential are independent of time, the gas is in *equilibrium*. When the temperature and the chemical potential depend on time, the gas is in *quasiequilibrium*. When the gas is observed on a time scale shorter than the particle scattering time, it may not have a definite temperature and a definite chemical potential in the kinetic-energy distribution because the gas is in *nonequilibrium*. For an ideal Bose gas, when the temperature falls down to a critical temperature, the chemical potential becomes zero and some of the particles in the gas condense to the ground state. This thermal statistical effect is recognized as a BEC phenomenon.

In this paper, in order to clarify how the exciton gas generated by the two-photon resonant absorption reaches equilibrium or quasiequilibrium from nonequilibrium, the orthoexcitonic gas in cuprous oxide is generated by one- and two-photon resonant absorption methods at different excitation intensities and at different temperatures between 1.8 and 4.2 K. The measured spectra are analyzed by simulation with a Boltzmann equation. It is found that the dynamics of the orthoexcitonic gas generated by the resonant excitation in cuprous oxide is mainly related to exciton-LA phonon scattering and exciton-exciton scattering. When the orthoexciton density is low, the exciton-LA phonon scattering is found to dominate the dynamics of the orthoexcitonic gas, and a luminescence from the nonequilibrium orthoexcitonic gas is observed, but the temperature and the chemical potential cannot be defined. On the contrary, when the orthoexciton density is high enough, the exciton-exciton scattering become so important that the observed luminescence is associated with orthoexcitons in a quasiequilibrium consisting of two systems: one following the usual Bose-Einstein statistics with chemical potential $\mu=0$, and the other originating from the excitons at an energy position corresponding to zero kinetic energy. Both systems proved to be in thermal equilibrium. The latter system might be a form of Bose-Einstein condensation.

II. EXPERIMENTAL PROCEDURES

The cuprous oxide crystal used in the measurements was prepared by a floating-zone technique using an infrared image furnace.[10,11] In the two-photon resonant excitation, we used a tunable infrared laser light with a pulse width of 7 ns and a repetition rate of 10 Hz from a Solar CF-151M color center laser. The infrared laser beam of 0.1–3 mJ/pulse with a cross-sectional diameter of 1 cm was focused through a lens with a 150-mm focal length onto a sample immersed in liquid helium whose temperature was controlled with a

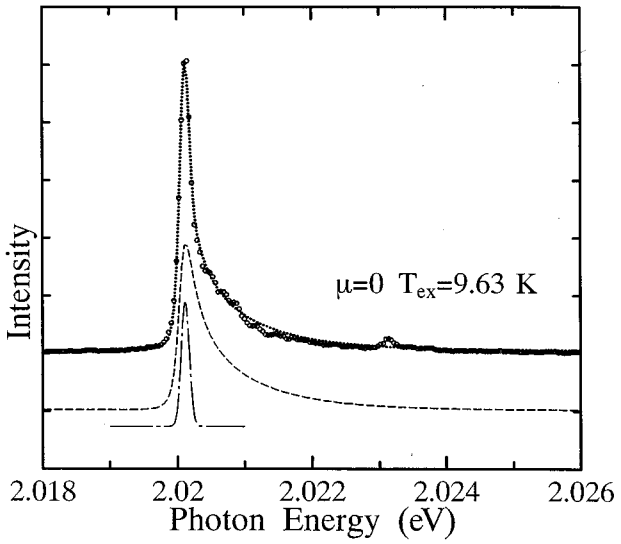

FIG. 1. Γ_{12}^{-} phonon-assisted luminescence spectrum at 1.8 K at a 20 ns delay after the infrared laser light whose power is stronger than 1 J/cm^2 per pulse and whose two-photon energy is the same as the orthoexcitonic energy. A broken line represents the usual Bose-Einstein statistics with a chemical potential $\mu=0$ and a temperature $T_{ex}=9.63$ K. A dash-dotted line represents the density of the zero-momentum excitons, and the linewidth shows the spectral resolution of the measurement system. A dotted line represents the sum of the broken line and the dash-dotted line. The peak intensities of the broken and dash-dotted curves are adjusted so that the peak of the dotted curve is fitted to the experimental points.

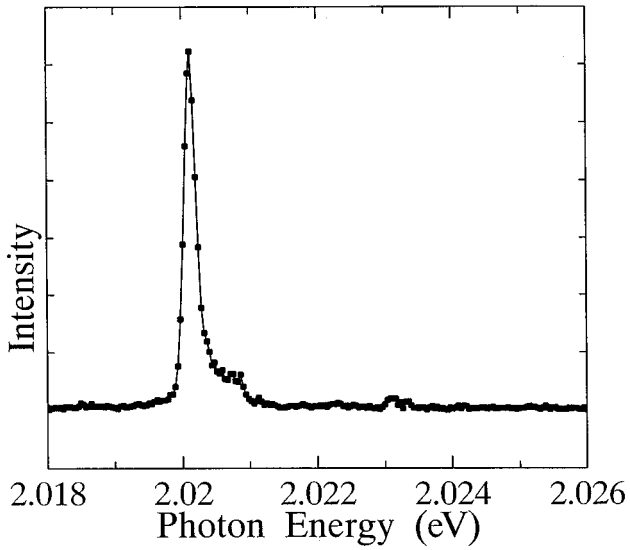

FIG. 2. Γ_{12}^{-} phonon-assisted luminescence spectrum at 1.8 K at a 20 ns delay after the incidence of an infrared laser light whose power is 20% of that in Fig. 1 and whose two-photon energy is the same as the orthoexcitonic energy. The spectral resolution is the same as that in Fig. 1.

vacuum pump and measured with a carbon register. The emitted light in the direction perpendicular to the infrared laser light was recorded by a charge-couple device (CCD) system with a spectrum resolution of 0.1 meV. For measuring the time-resolved luminescence spectra, an intensified circuit with a gate width of about 15 ns was set inside the CCD camera.

In the one-photon resonant excitation, the sample was excited by a Rhodamine B dye laser with a repetition rate of 76 MHz. The dye laser had a pulse width less than 10 ps and a power of 0.1 nJ/pulse. The emitted light in the direction perpendicular to the exciting light was analyzed by a monochromator with a spectral resolution of 0.15 meV and detected by a streak camera system with a resolution time less than 80 ps.

III. EXPERIMENTAL RESULTS

A. Two-photon resonant excitation

The circles in Fig. 1 show the luminescence spectrum of a Cu_2O crystal at 1.8 K at a 20 ns delay after excitation by an infrared laser light whose power is about 1 J/cm^2 per pulse on the crystal surface and whose two-photon energy is the same as the orthoexcitonic energy.[9] The main band is associated with the Γ_{12}^{-} phonon-assisted annihilation of the orthoexciton. The shape of the luminescence spectrum provides a direct way[4] to measure the velocity distribution of the nearly-free-exciton gas. The broken line represents the usual Bose-Einstein statistics[4,9] of the orthoexciton with a chemical potential $\mu=0$ and a temperature of 9.63 K. The dash-dotted line represents the density of zero-momentum excitons, and the linewidth shows the spectral resolution of the measurement system. The dotted line represents the sum of the broken line and the dash-dotted line whose peak intensities are adjusted to the experimental data. In our previous work,[9] we have already argued that the luminescence spectrum may be due to a thermal effect, i.e., the luminescence originates from a quasiequilibrium orthoexcitonic gas, and the dash-dotted part might be associated with the BEC. The reason why the temperature (9.63 K in Fig. 1) of the orthoexciton is higher than the bath temperature (1.8 K in Fig. 1) is as follows: When the orthoexciton decays into the paraexciton, a large number of phonons are generated, making the lattice temperature higher than the bath temperature. In addition to this phonon scattering, an Auger effect (well reported in Ref. 8) can also lead to heating of the crystal.

The statistical properties of boson gas change as the density or the temperature changes. A change in the excitation intensity (i.e., the orthoexciton density) or in the temperature may help us to clarify how the orthoexciton gas reaches an equilibrium or a quasiequilibrium from a nonequilibrium. The luminescence band shape depends on the excitation power. When the pump power is higher than about half the pump power in Fig. 1, the spectra can be fitted to a Bose distribution. And when the pump power is less than half the pump power in Fig. 1, an obvious small peak or shoulder appears at about 0.6 meV above the zero-momentum position, as shown in Fig. 2. This structure is caused by exciton-phonon scattering; the details will be described later. The temperature dependence of the luminescence spectrum is shown in Fig. 3. Except for the temperature, the experimental conditions are the same as in Fig. 1. As the temperature rises, the intensity of the higher-energy structure increases in comparison with that of the sharp peak at the zero-momentum position.

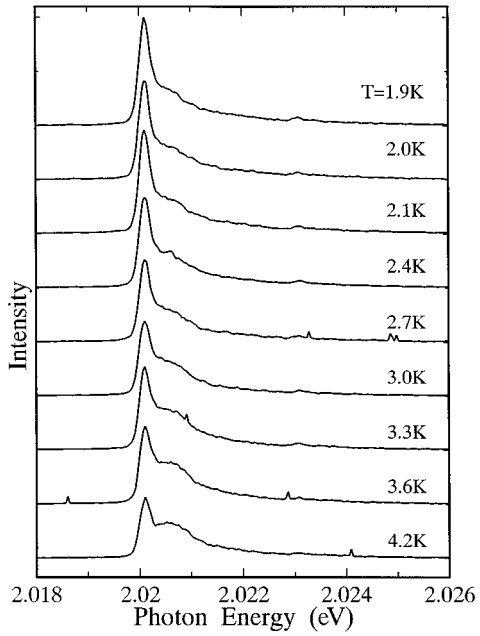

FIG. 3. The temperature dependence of the Γ_{12}^{-} phonon-assisted luminescence spectrum between 1.9 and 4.2 K at a 20 ns delay after the incidence of an infrared laser light whose power is similar to that in Fig. 1 and whose two-photon energy is the same as the orthoexcitonic energy. The spectral resolution is the same as that in Fig. 1.

Figure 4 shows the time-resolved spectra of the Γ_{12}^{-} phonon-assisted luminescence at 4.2 K when the crystal is excited resonantly to the orthoexciton energy by two photons. The excitation power is similar to that in Fig. 1. The delay times after the incidence of the infrared laser light are shown in this figure. The sharp lines (except for the 2.0202-eV line) originate from cosmic rays. The peak intensity at a position of about 0.6 meV above the zero-momentum position 2.0202 eV increases in comparison with that of the sharp peak at the zero-momentum position as the delay time becomes longer.

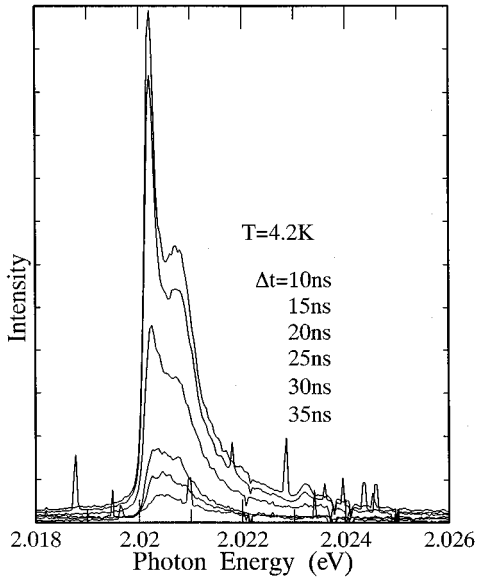

FIG. 4. Time-resolved spectra of the Γ_{12}^{-} phonon-assisted luminescence at 4.2 K at different delay times after the incidence of an infrared laser light whose power is similar to that of Fig. 1 and whose two-photon energy is the same as the orthoexcitonic energy. The spectral resolution is the same as that in Fig. 1. The zero delay is the same as that in Fig. 3 of Ref. 9.

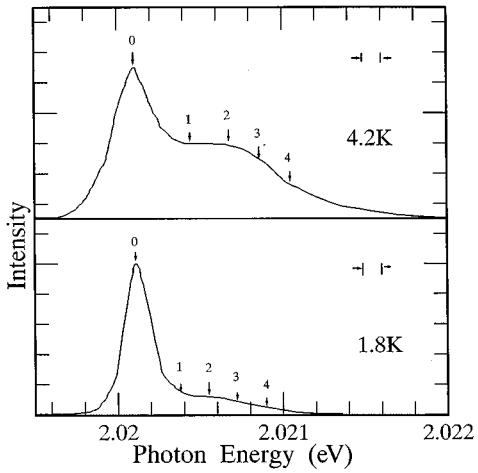

FIG. 5. Time-integrated Γ_{12}^{-} phonon-assisted emission spectra at 4.2 and 1.8 K. The crystal is excited by a Rhodamine B dye laser light whose photon energy is the same as the orthoexcitonic energy. The numbers 0,1,... represent the energy positions of the luminescences in Figs. 6 and 7.

The above phenomena are related to particle scatterings, which are the decisive feature of exciton dynamics. The scatterings occur so fast that a nanosecond system is not suitable for the study of these scatterings. In the following, a picosecond system is used to study the scattering dynamics.

B. One-photon resonant excitation

We directly generated nearly zero-momentum orthoexciton gas by one-photon resonant excitation as we did not have a tunable infrared picosecond pulsed laser with a narrow spectral width. The one-photon absorption was electric-quadrupole allowed and electric-dipole forbidden, and hence high-density orthoexciton gas was not generated. The time resolution, however, was greatly improved.

Figure 5 shows the time-integrated Γ_{12}^{-} phonon-related emission spectra at 1.8 and 4.2 K when the crystal is excited by a Rhodamine B dye laser light with the same photon energy as the orthoexcitonic energy. Figure 6 shows time decays of the luminescence at the peak position at 1.8 and 4.2 K, in the lower and upper parts, respectively. The measured pulse shape of the excitation laser light is shown in the figure, and the pulse width represents the time resolution of the system. The luminescence intensities decay single exponentially with the decay times of 1200 and 310 ps at 1.8 and 4.2 K, respectively. No component with the same shape as the laser pulse is found in the luminescence decay profiles. This fact shows clearly that the resonant Raman scattering component[12–16] is negligible in the emission spectra of Fig. 5. Raman scattering is a nonlinear optical effect whose decay time is as quick as that of the laser pulse.[16,17] Thus, nearly zero-momentum orthoexcitonic gas with a low density is directly generated and then annihilated radiatively with Γ_{12}^{-}

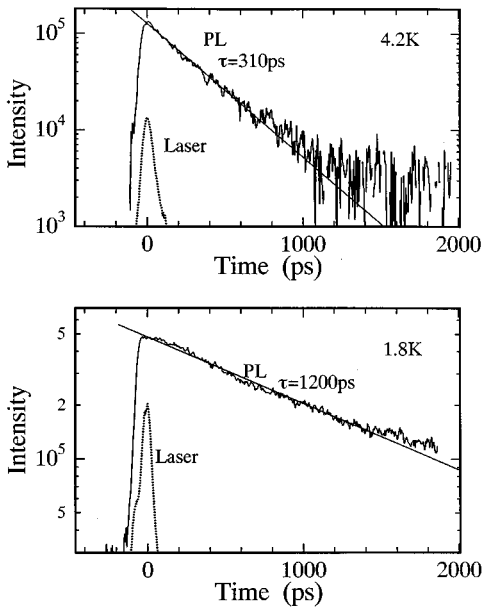

FIG. 6. The upper and lower curves show the time decays of the luminescences at the peak energy 0 in Fig. 5 at 4.2 and 1.8 K, respectively. The straight lines show exponential decays with 310 and 1200 ps at 4.2 and 1.8 K, respectively. The dotted lines are the excitation light pulses measured, and the pulse width represents the time resolution of the system.

phonon emission. The upper and lower parts of Fig. 7 show the time responses of the Γ_{12}^{-} phonon-assisted luminescence at different energy positions in the 1.8 and 4.2 K spectra, respectively, of Fig. 5. The corresponding photon energies are shown by numbers in Figs. 5 and 7. Figure 8(a) shows the time-resolved luminescence spectra at 4.2 K. The delay times are shown on the right side of this figure.

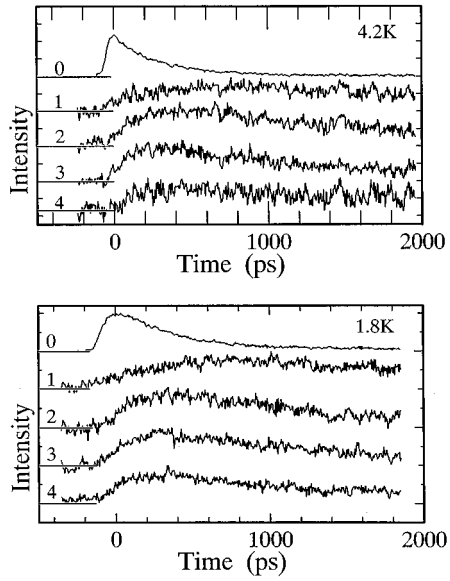

FIG. 7. The time decay curves of the luminescences with the different energies labeled in Fig. 5. The upper and the lower curves show the decay at 4.2 and 1.8 K, respectively.

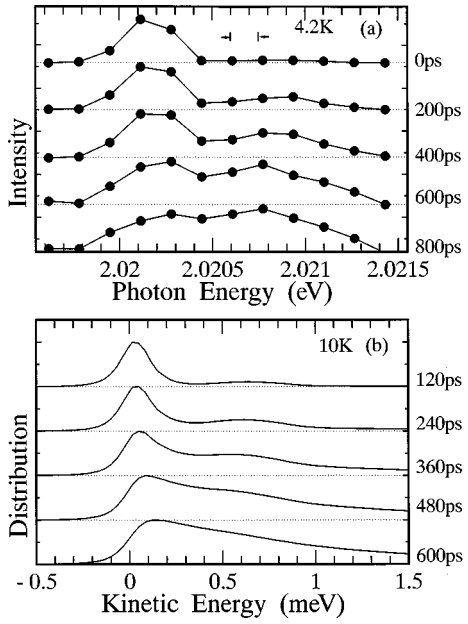

FIG. 8. (a) Time-resolved luminescence spectra at 4.2 K in one-photon excitation by Rhodamine B dye laser light. (b) Time-resolved luminescence spectra simulated with a Boltzmann equation including only exciton–LA-phonon interactions at a lattice temperature of 10 K.

IV. DISCUSSION

Exciton-exciton and exciton-phonon scatterings are the main processes in the dynamics of orthoexcitons. Exciton-exciton scattering depends on the exciton density. The exciton-exciton scattering becomes quicker with increasing exciton density. The exciton-phonon scattering does not depend on the exciton density when the exciton density is so low that the boson effect can be neglected (see Eqs. (2) and (3), the matrix elements for the exciton-phonon scattering, in this paper). In one-photon resonant excitation, the exciton-phonon scattering may be dominant as the exciton density is low.[18] In strong two-photon resonant excitation, both the exciton-exciton and the exciton-phonon scattering may be important.

From the temporal behavior of the luminescence in Fig. 7, we see that the rise time (about 100 ps) at the shoulder positions 2, 3, and 4, about 0.6 meV above the zero-momentum position 0, is much shorter than that (about 1000 ps) at position 1. This may be associated with the orthoexcitons with zero kinetic energy being scattered by phonons to orthoexcitons with nonzero kinetic energy and then the scattered excitons relaxing to a state of lower kinetic energy. Scattering by LA phonons is much more important than that by other phonons. The interaction between the exciton and the TA phonon is much weaker than that between the exciton and the LA phonon.[18] The optical-phonon scattering associated with phonon absorption can be neglected because the number of optical phonons is very small at this low temperature, and the optical-phonon scattering associated with phonon emission can also be neglected because of the small kinetic energy of the exciton in comparison with the optical-phonon energy. Thus we take into account only the LA-phonon scattering. In this scattering, both the momentum p and the en-

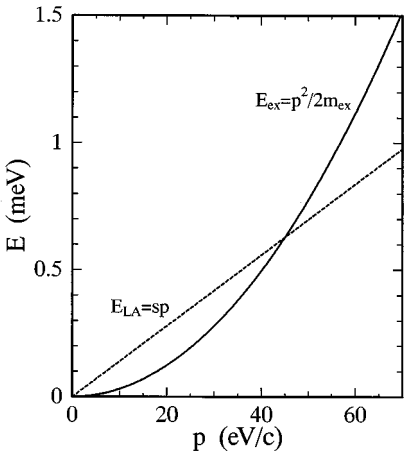

FIG. 9. The solid curve represents the kinetic energy of the exciton $E_{ex}=p^2/2m_{ex}$, where p is the momentum of the exciton, and m_{ex} is the exciton mass. The broken curve represents the LA-phonon energy $E_{LA}=sp$, where s is the velocity of the LA phonon, and $p=\hbar k$ is the momentum of the LA phonon. The two curves cross at an energy position of about 0.6 meV.

ergy E should be conserved. The solid and broken lines of Fig. 9 show the kinetic energies of the exciton and the LA phonon, E_{ex} and E_{LA}, respectively, as a function of the momentum p. The conservation rule holds at about 0.6 meV (the across point of the two curves), which agrees with the experimental results in Figs. 2, 3, 4, and 5, i.e., the energy difference between the peak and the high-energy side band.

The details of the LA-phonon scattering procedure are clarified by simulation with a Boltzmann equation.[18] The time derivative of the exciton number n with energy ε_k due to the LA phonon emission and absorption is given by the Boltzmann equation:

$$\begin{aligned}\frac{dn(\varepsilon_k)}{dt}=&\frac{2\pi}{\hbar}\frac{V}{(2\pi)^3}\int d^3q|M_{k+q,q}|^2 n(\varepsilon_{k+q})\\&\times\delta(\varepsilon_{k+q}-\varepsilon_k-\hbar\nu q)-\frac{2\pi}{\hbar}\frac{V}{(2\pi)^3}n(\varepsilon_k)\\&\times\int d^3q|M_{k,q}|^2\delta(\varepsilon_k-\varepsilon_{k-q}-\hbar\nu q)\\&+\frac{2\pi}{\hbar}\frac{V}{(2\pi)^3}\int d^3q|M'_{k-q,q}|^2 n(\varepsilon_{k-q})\\&\times\delta(\varepsilon_{k-q}+\hbar\nu q-\varepsilon_k)-\frac{2\pi}{\hbar}\frac{V}{(2\pi)^3}n(\varepsilon_k)\\&\times\int d^3q|M^1_{k,q}|^2\delta(\varepsilon_k+\hbar\nu q-\varepsilon_{k+q}),\end{aligned}\tag{1}$$

where

$$|M_{k,q}|=\frac{\hbar\Xi^2 q}{2\rho s V}(1+f_{k-q})(1+F_q),\tag{2}$$

$$|M'_{k,q}|=\frac{\hbar\Xi^2 q}{2\rho s V}(1+f_{k-q})F_q.\tag{3}$$

The first and second terms stand for the phonon emission, and the third and fourth terms stand for the phonon absorption. Ξ ($=1.8$ eV) is the deformation potential, i.e., the effective change in energy per unit strain, s is the LA phonon velocity, V the crystal volume, ρ the density of cuprous oxide, f_k the average occupation number of excitons with momentum $\hbar k$, and F_q the average occupation number of phonons with momentum $\hbar q$. As the exciton density in one-photon excitation is low, the $(f+1)$ in Eqs. (2) and (3) can be approximated to be unity in the calculation.[18]

If we choose the lattice temperature as 10 K, the exciton density distributions calculated from Eq. (1) can be shown in Fig. 8(b) as a function of the kinetic energy. From the fact that the calculated spectra [Fig. 8(b)] are similar to the experimental spectra [Fig. 8(a)], it is concluded that the LA-phonon scattering is very important in the case of one-photon excitation.

It is difficult to know in detail the local lattice temperature because many phonons may be generated by the orthoexciton decay into the paraexciton and the local lattice temperature may be higher than the bath temperature. The local temperature may depend on the time elapsed after the pulsed light excitation. In our previous work,[9] the excitonic temperature decreased from 10 to 4 K with increasing time. The change of the local lattice temperature may explain the slight disagreement between Figs. 8(a) and 8(b). Simulated spectra at different lattice temperatures show that exciton–LA-phonon scattering becomes more frequent with an increase in the lattice temperature. Thus, from the fact that the luminescence decay time of the zero-momentum orthoexciton is 310 ps at 4.2 K and 1200 ps at 1.8 K as shown in Fig. 6, it is suggested that the lifetime is mainly determined by the LA-phonon–exciton scattering.

Therefore, the above analysis leads to the conclusion that some of the nearly zero-momentum excitons created by the resonant photon absorption are scattered to non-zero-momentum excitons (with the average kinetic energy of about 0.6 meV) by the LA phonons, and then the exciton system reaches thermal equilibrium.

If the exciton-exciton scattering occurs frequently, a quasiequilibrium state is reached within the lifetime of the orthoexcitons. Here we take only the elastic exciton-exciton scattering process into account. Snoke and co-workers[19] used a Boltzman equation similar to Eq. (1) to simulate the effect of elastic carrier-carrier scattering on the kinetic-energy distribution. They found that a washing out of sharp features in the kinetic-energy distribution occurs on time scales of scores of τ. Here, τ is the average time of the carrier-carrier collision. τ can be estimated with the classical rate formula for hard spheres as

$$\tau=\frac{1}{n\sigma v},\tag{4}$$

where n is the density, v is the average velocity estimated from the excitonic temperature, and σ is the scattering cross section whose radius is about twice the Bohr radius of the exciton.[20] In the case of Fig. 1, n is estimated to be $\sim 10^{18}$ cm^3 and the temperature is about 10 K, as in our previous work.[9] The exciton-exciton collision time τ estimated from Eq. (4) is only several picoseconds. Therefore,

the excitonic system can quickly reach a quasiequilibrium made up of two states: excitons following the usual Bose-Einstein statistics with chemical potential $\mu=0$, and the energy state corresponding to zero kinetic energy.

On the one hand, the probability of the resonant two-photon absorption is proportional to $1/\Gamma^2$, where Γ is the homogeneous width of the orthoexciton energy. This width increases as the lattice temperature rises.[21] Thus the photogenerated orthoexciton density becomes lower as the lattice temperature rises. On the other hand, the nonradiative conversion rate from the orthoexciton to the paraexciton is proportional to $T^{3/2}$ in the low-temperature range.[22,23] This process means that the density of the orthoexciton becomes lower as the temperature rises. Therefore, the orthoexciton density n in the case of Fig. 4 at 4.2 K is lower than that in the case of Fig. 1 at 1.8 K, even under a similar excitation power. Thus in Fig. 4, the exciton-exciton scattering is not fast enough to allow the orthoexciton system to reach a quasiequilibrium. As a result, the small peak or shoulder at about 0.6 meV above the zero-momentum position is observed.

Taking into account the effects of the temperature dependence of the two-photon absorption probability, the conversion rate from the orthoexciton to the paraexciton, and the orthoexciton–LA-phonon scattering, it is understood that in Fig. 3, as the temperature rises, the intensity of the peak or shoulder increases in comparison with that of the sharp peak at the zero-momentum position.

The appearance of the small peak or shoulder means that the exciton system has not reached quasiequilibrium yet.

Comparing Fig. 4 of the present paper with Fig. 3 in Ref. 9 of our previous work, we notice that in the case of high exciton density (the latter figure), the zero-kinetic-energy component lasts more than 30 ns in contrast to about 20 ns in the case of lower exciton density (the former figure). This fact is contrary to what one would expect classically, and hence it gives us strong evidence that the two components in Fig. 1 are associated with two exciton systems in thermal equilibrium. Therefore we think that the zero-kinetic-energy component in Fig. 1 might be a form of the Bose-Einstein condensation.

V. SUMMARY

It was found that the exciton–LA-phonon and exciton-exciton scatterings are fundamental in the dynamics of orthoexciton gas generated by resonant excitation in cuprous oxide. Nearly zero-momentum orthoexcitons can be directly generated by both two-photon and one-phonon resonant absorptions. The two-photon resonant excitation can generate high-density orthoexcitons and allow us to study their quantum statistics. The one-photon resonant excitation can only generate low-density orthoexcitons, but this method allows us to study the fast processes associated with reaching thermal equilibrium. Some of the nearly zero-momentum orthoexcitons generated are scattered by LA phonons to finite-momentum excitons whose average kinetic energy is about 0.6 meV. When the density of the orthoexciton is low, the exciton-exciton scattering is not frequent, and hence, the exciton gas cannot reach even quasiequilibrium in a time range of several hundred picoseconds. In this case, a small peak or shoulder is observed at a position of 0.6 meV above the zero-momentum position in the luminescence spectra. When the density of the orthoexciton is very high in two-photon resonant excitation at 1.8 K, the exciton-exciton scattering is so frequent that the orthoexciton gas can reach a quasiequilibrium where the chemical potential and the temperature are definable. The luminescence band consists of two states: one follows the usual Bose-Einstein statistics with the chemical potential $\mu=0$, and the other is located at an energy state corresponding to zero kinetic energy. The latter state lasts a few tens of nanoseconds after the excitation laser pulse, and lasts longer when the density is higher. This is not expected classically, and hence, gives strong evidence that the two exciton systems are in thermal equilibrium. Thus the latter state might be attributed to Bose condensed excitons, and luminescence study by two-photon resonant absorption at low temperatures may provide an interesting way to study Bose-Einstein condensation of orthoexcitons in cuprous oxide.

ACKNOWLEDGMENTS

This work was supported by a Grant-in-Aid for Scientific Research from the Ministry of Education, Science and Culture of Japan. We are grateful to Mr. M. Saito of Tohoku University for technical assistance.

[1] M. H. Anderson, J. R. Ensher, M. R. Mattews, C. E. Wieman, and E. A. Cornell, Science **269**, 198 (1995); C. C. Bradley, C. A. Sackett, J. J. Tollett, and R. G. Hulet, Phys. Rev. Lett. **75**, 1687 (1995); K. B. Davis, M. Mewes, M. R. Andrews, N. J. Druten, D. S. Durfee, D. M. Kurn, and W. Ketterle, *ibid.* **75**, 3969 (1995).

[2] J. Lin and J. P. Wolfe, Phys. Rev. Lett. **71**, 1222 (1993).

[3] A. Compaan and H. Z. Cummins, Phys. Rev. B **6**, 4753 (1972).

[4] D. Hulin, A. Mysyrowicz, and C. Benoit a la Guillaume, Phys. Rev. Lett. **45**, 1970 (1980).

[5] D. Snoke, J. P. Wolfe, and A. Mysyrowicz, Phys. Rev. Lett. **59**, 827 (1987).

[6] D. W. Snoke, J. P. Wolfe, and A. Mysyrowicz, Phys. Rev. B **41**, 11 171 (1990).

[7] N. Naka, S. Kono, M. Hasuo, and N. Nagasawa, Prog. Cryst. Growth Charact. **33**, 89 (1996).

[8] G. M. Kavoulakis, Gordon Baym, and J. P. Wolfe, Phys. Rev. B **53**, 7227 (1996).

[9] T. Goto, M. Y. Shen, S. Koyama, and T. Yokouchi, Phys. Rev. B **55**, 7609 (1997). This paper includes an error: in Fig. 5 on page 7613, the experimental points in the lower excitation power range less than half the maximum are incorrect. The correct points follow the solid curve. This means that the luminescence intensity is proportional to the orthoexciton density in the whole

power range. The coherency effect resulting in increase of the luminescence intensity has not been observed. The correct data support the viewpoint that the two-photon resonant absorption at low temperatures provides a way for studying Bose-Einstein condensation of the orthoexciton in cuprous oxide.

[10] D. Trivich and G. P. Pallack, J. Electrochem. Soc. **117**, 344 (1970).

[11] W. S. Brower, Jr. and H. S. Parker, J. Cryst. Growth **8**, 227 (1971).

[12] A. Compaan and H. Z. Cummins, Phys. Rev. Lett. **31**, 41 (1973).

[13] A. Z. Genack, H. Z. Cummins, M. A. Washington, and A. Compaan, Phys. Rev. B **12**, 2478 (1975).

[14] M. A. Washington, A. Z. Genack, H. Z. Cummins, R. H. Bruce, A. Compaan, and R. A. Forman, Phys. Rev. B **15**, 2145 (1977).

[15] Peter Y. Yu and Y. R. Shen, Phys. Rev. B **17**, 4017 (1978).

[16] J. S. Weiner and P. Y. Yu, Solid State Commun. **50**, 493 (1984).

[17] Y. R. Shen, Phys. Rev. B **9**, 622 (1974).

[18] D. W. Snoke, D. Braun, and M. Cardona, Phys. Rev. B **44**, 2991 (1991).

[19] D. W. Snoke and J. P. Wolfe, Phys. Rev. B **39**, 4030 (1989); D. W. Snoke, W. W. Ruhle, Y. Lu, and E. Bauser, *ibid.* **45**, 10 979 (1992).

[20] E. Hanamura and H. Haug, Phys. Rep. **33**, 209 (1977).

[21] In the work of D. W. Snoke, A. J. Shields, and M. Cardona, Phys. Rev. B **45**, 11 693 (1992), the spectral broadening with temperature rising was measured at higher temperature range where optical phonons are of importance (an Einstein model). In the present work, at low-temperature range, the acoustic phonons are of importance (a Debye model).

[22] N. Caswell and P. Y. Yu, Phys. Rev. B **25**, 5519 (1982).

[23] J. S. Weiner, N. Caswell, P. Y. Yu, and A. Mysyrowicz, Solid State Commun. **46**, 105 (1983).